Received: 16 August 2018 | Revised: 25 February 2019 | Accepted: 15 March 2019

DOI: 10.1002/epi4.12318

FULL-LENGTH ORIGINAL RESEARCH

Epilepsia Open® Open Access

Interictal epileptogenic zone localization in patients with focal epilepsy using electric source imaging and directed functional connectivity from low-density EEG

Ana Coito[1] | Silke Biethahn[1] | Janina Tepperberg[1] | Margherita Carboni[2] | Ulrich Roelcke[3] | Margitta Seeck[2] | Pieter van Mierlo[4] | Markus Gschwind[1] | Serge Vulliemoz[2]

[1]Department of Neurology, Cantonal Hospital Aarau, Aarau, Switzerland

[2]Department of Neurology, University Hospital Geneva, Geneva, Switzerland

[3]Department of Neurology and Brain Tumor Center, Cantonal Hospital Aarau, Aarau, Switzerland

[4]Department of Electronics and Information Systems, Ghent University, Ghent, Belgium

Correspondence
Serge Vulliémoz, Department of Neurology, University Hospital Geneva, Geneva, Switzerland.
Email: Serge.Vulliemoz@hcuge.ch

Funding information
Cantonal Hospital of Aarau (KSA), Grant/Award Number: 1410.000.084; Schweizerischer Nationalfonds zur Förderung der Wissenschaftlichen Forschung, Grant/Award Number: 163398, CRSII5_170873 and 320030-169198; Marie Sklodowska-Curie, Grant/Award Number: 660230

Summary

Objective: Electrical source imaging (ESI) is used increasingly to estimate the epileptogenic zone (EZ) in patients with epilepsy. Directed functional connectivity (DFC) coupled to ESI helps to better characterize epileptic networks, but studies on interictal activity have relied on high-density recordings. We investigated the accuracy of ESI and DFC for localizing the EZ, based on low-density clinical electroencephalography (EEG).

Methods: We selected patients with the following: (a) focal epilepsy, (b) interictal spikes on standard EEG, (c) either a focal structural lesion concordant with the electroclinical semiology or good postoperative outcome. In 34 patients (20 temporal lobe epilepsy [TLE], 14 extra-TLE [ETLE]), we marked interictal spikes and estimated the cortical activity during each spike in 82 cortical regions using a patient-specific head model and distributed linear inverse solution. DFC between brain regions was computed using Granger-causal modeling followed by network topologic measures. The concordance with the presumed EZ at the sublobar level was computed using the epileptogenic lesion or the resected area in postoperative seizure-free patients.

Results: ESI, summed outflow, and efficiency were concordant with the presumed EZ in 76% of the patients, whereas the clustering coefficient and betweenness centrality were concordant in 70% of patients. There was no significant difference between ESI and connectivity measures. In all measures, patients with TLE had a significantly higher ($P < 0.05$) concordance with the presumed EZ than patients with with ETLE. The brain volume accepted for concordance was significantly larger in TLE.

Significance: ESI and DFC derived from low-density EEG can reliably estimate the EZ from interictal spikes. Connectivity measures were not superior to ESI for EZ localization during interictal spikes, but the current validation of the localization of connectivity measure is promising for other applications.

Gschwind and Vulliemoz contributed equally to this work and shared last authroship..

KEYWORDS
directed functional connectivity, electrical source imaging, epileptogenic zone, focal epilepsy, low-density EEG

1 | INTRODUCTION

In patients with focal epilepsy that is refractory to antiepileptic drugs,[1] epilepsy surgery can be a very efficient treatment. Therefore, the accurate location of the cortical areas to be removed by surgery (epileptogenic zone, EZ) is crucial. The localization of the EZ is often difficult and requires concordant results of several presurgical evaluation techniques. For that purpose, the development of new noninvasive diagnostic and prognostic markers is necessary.

The high temporal resolution of electroencephalography (EEG) allows for the study of pathologic brain activity, such as interictal spikes and seizures, and analysis of their temporal dynamics. For each time point of the EEG signal, we can reconstruct the source activity that underlies what is measured on the scalp using electrical source imaging (ESI).[2] Studies have shown that ESI can reliably localize the seizure-onset zone and the irritative zone.[3–5] State-of-the-art ESI for epilepsy presurgical evaluation is performed using high-density EEG recordings (96-256 channels), which are not yet widely available. ESI applied to standard clinical recordings (long-term or short duration) is less accurate compared to high density but can nevertheless yield clinically useful information.[3,6,7]

There is an increasing consensus that epilepsy involves large-scale brain networks rather than single sources.[8,9] A better understanding about the interactions between brain regions is crucial for understanding this disorder and could provide important diagnostic and prognostic information. These interactions can be studied using measures of functional connectivity that estimate how the activity of one brain region is related to another. We have recently developed a methodologic approach for studying directed functional connectivity (DFC) based on high-density EEG and ESI, to investigate directional information flow between brain regions.[10] First, ESI is performed to estimate the brain source activity in each region. Then, directional functional interactions between the activity of all brain regions are derived using the concept of Granger causality.[11] We showed that left temporal lobe epilepsy (LTLE) and right TLE (RTLE) involve very different network alterations in terms of the main drivers of information flow during interictal spikes[12] and also in the absence of visible epileptic activity.[13] Recent evidence from ictal recording suggests a high localization value for functional connectivity applied to low-density ictal recordings.[14]

In this study, we investigate whether ESI and DFC can correctly localize the EZ in patients with focal epilepsy (TLE and extra-TLE, ETLE) during interictal spikes, based on clinical recordings (21-38 electrodes). We investigated whether the identified regions with highest source activity and connectivity (summed outflow, clustering coefficient, betweenness centrality, and efficiency) were inside the presumed EZ, defined as the resection area in patients who were seizure-free after surgery, or the epileptogenic lesion in patients who did not undergo surgery.

Key Points

- Electrical source imaging (ESI) and connectivity analysis can estimate the epileptogenic zone (EZ) from interictal spikes recorded with low-density electroencephalography (EEG)
- Higher concordance with the presumed EZ in temporal lobe epilepsy (TLE) than extra-TLE (ETLE)
- No significant difference between ESI and connectivity measures for localization of the EZ

2 | METHODS

2.1 | Subjects

We searched in the database of the Cantonal Hospital of Aarau and the University Hospital of Geneva for patients with epilepsy who fulfilled the following criteria: (a) focal epilepsy; (b) focal magnetic resonance imaging (MRI) lesion; (c) invasively well-characterized presumed EZ (focal structural lesion concordant with electroclinical semiology) or localization of the EZ confirmed by good surgical outcome (Engel class I = International League Against Epilepsy [ILAE] 1 or 2); and (d) presence of ≥10 interictal epileptic discharges of the same (single) type on low-density EEG. Patients with multifocal interictal epileptic discharges were not included.

We included 34 patients in this study (mean age ± standard deviation 32.82 ± 15.12 years; 15 women), 20 with TLE and 14 with ETLE. The patient's clinical information is provided in Table 1.

The gold-standard for EZ localization was defined as (a) the volume removed by surgery in postoperatively seizure-free patients and (b) the cortical lesion concordant with electroclinical semiology, in patients who did not undergo surgery.

TABLE 1 Patients' clinical details

	Gender	Age	Age at onset	Disease duration	Presumed EZ	MRI lesion	Number of spikes	Spike maximum	Surgery outcome (Engel)	icEEG	Number of EEG electrodes
P1	F	47	25	22	Left temporal	HS	35	T1	I	No	21
P2	F	46	12	34	Right temporal	HS	97	T2	I	No	21
P3	M	19	3	16	Right temporal	HS	113	T2	I	No	21
P4	M	20	4	16	Right frontoparietal	Abscess scar	37	C4	I	No	21
P5	F	38	34	4	Left frontal	Meningioma	33	C3	I	No	21
P6	M	18	8	10	Left temporal	Normal	31	P7	I	Yes	29
P7	M	76	73	3	Right frontal	Meningioma	13	F4	No surgery	No	19
P8	F	21	16	5	Right parieto-occipital	Intracerebral hemorrhage	68	T6	No surgery	No	19
P9	F	18	11	7	Left parietal	FCD	132	T5	I	Yes	37
P10	M	45	44	1	Right frontal	Porencephaly	45	T2, T4, F8	No surgery	No	19
P11	M	29	26	3	Left temporal	DNET	20	T3	I	No	21
P12	M	15	1	14	Left temporal	FCD	29	T1	I	No	31
P13	M	16	11	5	Right temporal	HS	29	T2, Tp10	I	Yes	31
P14	M	35	22	13	Right temporal	Normal	38	T2	No surgery	Yes	31
P15	M	27	5	22	Right temporal	HS	33	T2, F8	I	No	21
P16	M	30	30	0	Right basal frontal	Teratoma	10	F8	I	No	21
P17	M	35	25	10	Right frontal	FCD	48	F4, F8	II	NO	37
P18	F	31	28	3	Right central	Anaplastic astrocytoma WHO gr III	18	T4	No surgery	No	21
P19	M	15	11	4	Left temporal	HS	49	F7	I	No	29
P20	M	35	33	2	Right temporal	HS	65	T2, F8	I	Yes	31
P21	M	18	13	5	Left temporal	Normal	68	T7, F7	I	Yes	29
P22	F	21	5	16	Left temporal	HS	29	F7, Fp1	I	No	31
P23	F	32	9	23	Right temporal	HS	19	T2, F8	I	Yes	31
P24	F	46	3	43	Left temporal	HS	35	F7, Fp1	I	No	29
P25	F	43	20	23	Right temporal	HS	29	T2, F8	II	No	31
P26	F	28	14	14	Right temporal	Normal	11	F8, Fp2	I	Yes	29
P27	M	10	4	6	Right parietal	Normal	118	FC6, T8	I	Yes	31
P28	M	29	15	14	Right temporal	Cavernoma	37	T8	I	No	21

(Continues)

TABLE 1 (Continued)

	Gender	Age	Age at onset	Disease duration	Presumed EZ	MRI lesion	Number of spikes	Spike maximum	Surgery outcome (Engel)	icEEG	Number of EEG electrodes
P29	F	55	41	14	Left parietal	FCD	59	P3, CP1	I	No	31
P30	M	18	8	10	Left temporal	HS	58	F7, T1, T7	I	No	31
P31	M	43	43	0	Right frontal	Astrocytoma WHO II	41	C4	II	No	21
P32	F	60	52	8	Left temporo-insular	Low-grade glioma	16	T1, T3	No surgery	No	21
P33	F	45	23	22	Right frontal	Craniopharyngioma, cavernoma	48	F4	I	No	21
P34	F	52	25	27	Right temporal	Normal	12	T4	I	Yes	31

DNET, dysembryoplastic neuroepithelial tumor; EZ, epileptogenic zone; F, female; FCD, focal cortical dysplasia; HS, hippocampal sclerosis; icEEG, intracranial EEG; M, male.

This study was approved by the local ethics committees of both hospitals.

2.2 | EEG preprocessing

Clinical EEG recordings of at least 10 minutes were considered and the numbers of channels were as follows: 19-channel recording (N = 3), 21 (N = 13), 29 (N = 5), 31 (N = 11), and 37 (N = 2).

The patients who underwent the 19-channel recording were all ETLE patients (Figure S1). The 21-channel montage included electrodes T1 and T2 (see the different montage setups in Figure S1).

Isolated interictal epileptiform discharges (IEDs; minimum 10), free of major artifacts, were marked by one of three expert neurophysiologists (S.B., J.T., S.V.). To avoid contamination/residual effects, only spikes occurring at least 1 second after the previous IED peak were included. Epochs of 700 msec around the maximal negativity of each IED (350 msec before and 350 msec after the IED) were selected. Offline, the EEG was band-pass filtered between 1 and 100 Hz using a non-causal filter (second order Butterworth low- and high-pass, −12 db/octave roll-off, computed linearly forward and backward, eliminating the phase shift, and with poles calculated each time to the desired cut-off frequency. This corresponds to an Infinite Impulse Response [IIR] filter with a zero-phase shift, and no ripples near the cutting frequency, as provided by Cartool). After average referencing all recordings were down-sampled to 250 Hz.

2.3 | Electrical source imaging

ESI was used to reconstruct the source activity underlying the distribution of scalp potentials, for each time point in each patient as in our previous studies.[10,12,13,15] ESI involves the computation of the forward model and the solution of the inverse problem.[2] The forward model describes how electrical currents in the brain produce the measured scalp potentials and it requires the use of an appropriate head model. Using the individual T1-weighted MRI, we built a patient-specific head model with a 1 mm × 1 mm × 1 mm resolution using the Finite Difference Method (FDM).[16] To this aim, the structural MRI was segmented into six different tissues classes: white matter, gray matter, cerebrospinal fluid, skull, air cavities, and scalp. A tissue label and a corresponding electrical conductivity was assigned to each voxel to compute the lead field matrices containing the scalp potentials that are generated by dipoles placed in the gray matter.

In the inverse problem, the electrical source distribution in the brain is estimated given the recorded scalp potentials and the forward model. Here, we used a distributed linear inverse solution, the standardized low-resolution brain electromagnetic tomography (sLORETA),[17] because it gives a smooth

solution well suited to localize the dipolar voltage maps during the spike, and because it has been used successfully in multiple previous interictal ESI studies.[16,18,19]

In some patients high-density EEG (hd-EEG)–based ESI was performed as part of the clinical work-up and the result was integrated in the context of the multimodal presurgical workup, on which clinical management (surgery) was decided. Note, that in this context, ESI was never used as a stand-alone criterion to determine surgical targets.

To reduce the dimensionality of the results, we parceled the gray matter of each patient into 82 regions of interest (ROIs) using the automated anatomic labeling (AAL) digital atlas as template,[20] which was coregistered to the patient's individual MRI using the inverse of the segmentation matrix obtained using the Statistical Parametric Mapping Software (SPM8; www.fil.ion.ucl.ac.uk/spm). The centroid of each ROI was considered representative of the source activity of that ROI and the subsequent analysis was carried out in 82 voxels per patient, as described previously.[10]

For each patient, we also computed the time-frequency distribution of the spectral power in the source space using the S-Transform (ST)[21] in each ROI, as described previously.[10]

2.4 | Directed functional connectivity

To estimate DFC for each time point of each epoch, we used the time-varying weighted Partial Directed Coherence (wPDC).[22–24] This algorithm is based on Granger causality[11] and estimates directed interactions between pairs of signals in the time-frequency domain using adaptive multivariate autoregressive models of an appropriate order.[22,23,25,26] The wPDC has been applied to animal data[24] and to source signals derived from high-density EEG during interictal spikes[12] and resting-state.[13] Here we used a model order of 5, based on previous studies.[12,13,27] For each patient, a 5-dimensional connectivity matrix (ROIs × ROIs × frequency bins × time points × epochs) was obtained, representing the flow from one ROI to another at a certain frequency, time, and epoch. We then averaged the results across epochs. For each patient, we selected the time point of the peak of the spike, and the frequency corresponding to the maximum power for the ROI with the highest source activity during the spike. This resulted in a ROIs × ROIs matrix for each patient. Because our goal in the current study is to study the outflows, we used the normalization of wPDC with respect to the inflows.[24]

Based on this connectivity matrix, and in order to interpret and summarize the results, we computed several graph theory measures: the summed outflow, the clustering coefficient, the betweenness centrality, and the efficacy of the network. The summed outflow is the sum of all outgoing values from an ROI to all others. It reflects the driving importance of an ROI in the network, since ROIs with high summed outflow are supposed to strongly drive activity of other ROIs. The clustering coefficient is the number of connections that exist between neighbors of a node as a proportion of all possible connections.[28] The betweenness centrality quantifies the number of shortest paths between all node pairs that pass through that node.[28] The efficiency is the inverse of the shortest path length, which is the average minimum number of nodes that have to be crossed to go from one node to any other.[28] The clustering coefficient, betweenness centrality, and efficiency were computed at the time point of the spike peak using the weighted directed functions available in the Brain Connectivity Toolbox of Matlab.[29] All measures of ESI and connectivity were calculated on each time point and then averaged across all time points to obtain one value per patient and ROI.

2.5 | Concordance assessment for ESI and connectivity measures

The assessment of the performance of the method was done based on the "ground truth" established by the multimodal presurgical workup, on which clinical management (ie, surgery) was decided for each patient, comprising electroclinical semiology, positron emission tomography (PET), single-photon emission tomography (SPECT), intracranial and hd-EEG with subsequent ESI in some cases. ESI was never the only criterion to determine surgical targets.

For each of the investigated measures (ESI, summed outflow, betweenness centrality, clustering coefficient, and efficiency), we determined in how many patients the atlas-based ROI with the highest magnitude overlapped with the presumed EZ, using the results of the average ESI or summary connectivity obtained from all marked spikes in each patient, like in our previous studies.[10,12,13,15] The percentage (%) of concordant patients was computed for each of the measures. The same procedure was done separately for TLE and ETLE patients. A chi-square test was performed to assess differences between measures.

The effect of the size of the lesion or resection and the overlap with concordant ROIs was studied by calculating the number of concordant ROIs (overlapping with lesion/resection) and the percentage of total brain volume that they represented. In the four operated patients with no available postoperative MRI, we estimated concordance based on resection described in medical notes (N = 3, anterior temporal lobe resection; N = 1, amygdalohippocampectomy). To investigate whether the number of electrodes played a role in EZ estimation, we identified the patients who had an incorrect estimation for the different electrode setups and tested the difference using a chi-square test. Because of the explorative nature of this study we did not use correction for multiple comparisons (ESI, connectivity measures vs resection/lesion).

2.6 | Software

EEG preprocessing, epoch segmentation, and MRI parcellation were done using the freely available software *Cartool* (https://

TABLE 2 Regions of interest with the highest electrical source imaging (ESI), summed outflow, clustering coefficient, betweenness centrality. And efficiency for each patient

		ESI maximum		Summed outflow maximum		Clustering coefficient maximum		Betweenness centrality maximum		Efficiency maximum	
	Presumed EZ	Region	C/D	Region	C/D	Region	C/D	Region	C/D	Region	C/D
P1	Left temporal	Hipp-L	C	TPMid-L	C	TMid-R	C	OccInf-R	D	TMid-R	C
P2	Right temporal	TPMid-R	C	TPMid-R	C	TPMid-R	C	PHipp-R	C	PHipp-L	C
P3	Right temporal	Hipp-R	C	TInf-R	C	TInf-R	C	TInf-R	C	TInf-R	C
P4	Right parieto-frontal	PreC-R	C	PreC-R	C	FrInfOp-R	C	FrInfOp-R	C	FrInfOp-R	C
P5	Left frontal	PreC-L	C	PreC-L	C	PreC-L	C	PreC-L	C	Hipp-L	C
P6	Left temporal	Fus-L	C	Fus-L	C	Fus-L	C	Fus-L	C	Fus-L	C
P7	Right frontal	FrMid-R	C	FrMid-R	C	CingAnt-R	C	CingAnt-R	C	CingAnt-R	C
P8	Right parieto-occipital	OccInf-R	C	OccInf-L	C	OccInf-R	C	OccInf-R	C	ling-L	C
P9	Left parietal	Fus-L	D	OccInf-L	D	OccInf-L	D	OccInf-L	D	OccInf-L	D
P10	Right frontal	PHipp-R	D	Fus-R	D	Hipp-R	D	Olf-L	D	CingMid-L	D
P11	Left temporal	Amyg-L	C	TPSup-L	C	TPSup-L	C	TPSup-L	C	TPSup-L	C
P12	Left temporal	PHipp-L	C	TInf-L	C	TPMid-L	C	TPMid-L	C	TInf-L	C
P13	Right temporal	PHipp-R	C	TInf-R	C	TInf-R	C	TInf-R	C	TInf-R	C
P14	Right temporal	Amyg-R	C	TPMid-R	C	TPSup-R	C	Olf-R	D	TPSup-R	C
P15	Right temporal	Amyg-R	C	TPMid-R	C	Amyg-R	C	TPMid-R	C	TPMid-R	C
P16	Right frontal	FrInfOrb-R	C	FrInfOrb-R	C	FrInfOrb-R	C	FrInfOrb-R	C	FrInfOrb-R	C
P17	Right frontal	Olf-R	D	SMA-R	D	CingAnt-R	D	CingMid-R	D	SMA-R	D
P18	Right central	TPSup-R	D	TPSup-R	D	TPSup-R	D	TPSup-R	D	TPSup-R	D
P19	Left temporal	Amyg-L	C	Amyg-L	C	Amyg-L	C	PHipp-L	C	Amyg-L	C
P20	Right temporal	Amyg-R	C	Amyg-R	C	Amyg-R	C	Hipp-R	C	Amyg-R	C
P21	Left temporal	PHipp-L	C	Hipp-L	C	PHipp-L	C	Hipp-L	C	PHipp-L	C
P22	Left temporal	Amyg-L	C	Hipp-L	C	Hipp-L	C	Hipp-L	C	Hipp-L	C
P23	Right temporal	Amyg-R	C	TPSup-R	C	TPMid-R	C	TPMid-R	C	TPMid-R	C
P24	Left temporal	Olf-L	D	TPMid-L	C	TPMid-L	C	TPMid-L	C	TPMid-L	C
P25	Right temporal	PHipp-R	C	Amyg-R	C	Amyg-R	C	PHipp-R	C	Amyg-R	C
P26	Right temporal	PHipp-R	C	Hipp-R	C	Ling-R	D	Ling-R	D	Ling-R	D
P27	Right parietal operculum	RolOper-R	C	FrInfOp-R	D	FrInfOp-R	D	FrInfOp-R	D	FrInfOp-R	D
P28	Right temporal	Fus-R	D	Fus-R	D	Fus-R	D	Fus-R	D	Fus-R	D
P29	Left parietal	CingPost-L	D	PHipp-L	D	PHipp-L	D	CingMid-L	D	PHipp-L	D
P30	Left temporal	Hipp-L	C	TInf-L	C	Tinf-L	C	TInf-L	C	TInf-L	C
P31	Right frontal	HeG-R	D	HeG-R	D	HeG-R	D	CingMid-R	C	CingMid-R	C
P32	Left temporo-insular	Tinf-R	C	TInf-L	C	TPSup-L	C	TPSup-L	C	TInf-L	C
P33	Right frontal	FrInfTri-R	C	FrInfTri-R	C	FrInfTri-R	C	FrInfTri-R	C	FrInfTri-R	C
P34	Right temporal	Hipp-R	C	TSup-R	C	HeG-R	D	Fus-R	C	Fus-R	C

C/D, Concordance/discordance with presumed EZ; CingAnt, anterior cingulate cortex; CingMid, middle cingulate cortex; CingPost, posterior cingulate cortex; EZ, epileptogenic zone; FrInfOrb, orbital part of the inferior frontal gyrus; FrInfTri-R, triangularis part of the inferior frontal gyrus; FrMid, middle frontal gyrus; Fus, fusiform gyrus; HeG, Heschl gyrus; Hipp, hippocampus; L, left; Olf, olfactory gyrus; OccInf, inferior occipital gyrus; PHipp, parahippocampal gyrus; PreC, precentral gyrus; R, right; RolOper, rolandic operculum; TPMid, medial temporal pole; TPSup, superior temporal pole; TInf, inferior temporal gyrus.

sites.google.com/site/cartoolcommunity/). EEG source imaging comprising the inverse solution with sLORETA and the FDM head model was computed using software written in *Matlab* (Release 2012b, The MathWorks, Inc., Natick, MA), like in our previous studies.[16,30] The Matlab code has entered Epilog NV (Ghent, Belgium). Connectivity estimation was performed equally with in house software written in *Matlab,* like in our previous studies.[10,12,13,15]

3 | RESULTS

The mean dominating frequency of the estimated cortical activity during the time point of spikes in the ROI with strongest activity was 5.7 ± 2.0 Hz. This is to be expected as the spectrum of a peak, like an epileptic spike, is smeared across the frequency bins. The ROIs with highest amplitude obtained by ESI, summed outflow, clustering coefficient, betweenness centrality, and efficiency, for each patient and at the time point of the spike peak, as well as the concordance are shown in Table 2. ESI and summed outflow were both concordant in 32 of 34 patients.

The percentage of concordant patients for ESI was 76% (26/34) (90% in TLE and 57% in ETLE, $P = 0.026$). Concerning the connectivity measures, percentage of concordant patients for the summed outflow was also 76% (26/34) (95% in TLE and 50% in ETLE, $P = 0.002$), 70% (24/34) for the clustering coefficient (85% [29/34] in TLE and 50% [17/34] in ETLE, $P = 0.027$), 70% (24/34) for the betweenness centrality (80% in TLE and 57% in ETLE, $P = 0.15$), and 76% (26/34) for the efficiency (90% in TLE and 50% in ETLE, $P = 0.009$; Figure 1). Of interest, in two patients, ESI was discordant, whereas most connectivity measures were concordant and in two other patients, the reverse was found.

We did not find any statistically significant differences between ESI and the various connectivity measures for the concordance with the EZ ($P > 0.05$).

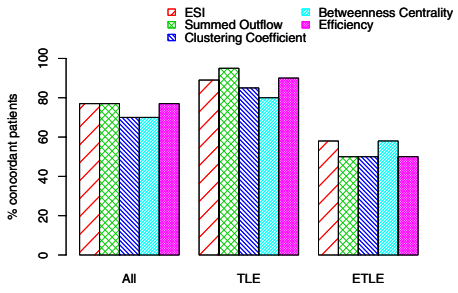

FIGURE 1 Concordance of localization estimated by the different measures (ESI, summed outflow, clustering coefficient, betweenness centrality, and efficiency) with the presumed epileptogenic zone.

Figure 2 shows two illustrative cases of the results for EEG, ESI, and summed outflow for one TLE and one ETLE patient.

3.1 | Effect of lobe

We found that lesions/resections in TLE overlapped with a larger number of ROIs in TLE than in ETLE patients (TLE: 2-8, median 8.0; ETLE: 1-6, median 3; Mann-Whitney U = 225; $P < 0.0001$) and therefore in TLE a larger percentage of source space volume was accepted as concordant than in ETLE (TLE: 1.3-9.6%, median 8.4%; ETLE 1.3-7.3%, median 3.2%; Mann-Whitney U = 223; $P < 0.0001$; Table S1 and Figure S1).

3.2 | Effect of number of channels

Table 3 shows the number of incorrect EZ localizations for each category of different channel numbers. A chi-square test showed no difference in the results with recordings using different number of channels ($P > 0.05$). In addition, when a chi-square test was performed in two separate groups—recordings with fewer than 25 channels and recordings with more than 25 channels—we verified that in 12 of 16 patients with fewer than 25 electrodes and in 14 of 18 patients with more than 25 electrodes, the localization was correct. This was not statistically significant ($P > 0.05$).

4 | DISCUSSION

Using low-density EEG, we showed that both ESI and DFC measures can reliably localize the EZ from interictal spikes in 90% of the TLE and 57% of the ETLE patients. We found no added value in the performance of connectivity measures vs ESI to localize the EZ. ESI and connectivity measures were concordant except in 2 of 34 patients. Finally, we showed that the different number of electrodes did not influence the localization in our patient group.

In this study, we used clinical EEG studies similar to those recorded during the standard evaluations in most epilepsy centers. Using ESI and, if possible, connectivity analysis to identify the EZ in a clinical setting would add a valuable additional diagnostic tool to help clinicians in the diagnosis of focal epilepsy. This is particularly useful in cases where the other currently available localization modalities are not concordant. Unlike visual analysis, ESI and connectivity measures offer an objective assessment of the regions that play a key role in the disease. Both ESI and DFC measures using high-density EEG (64-256 electrodes) have previously shown reliable results for EZ localization during interictal spikes.[3,12] Our study supports the reliability of ESI and DFC, also in interictal clinical low-density EEG recordings that are much

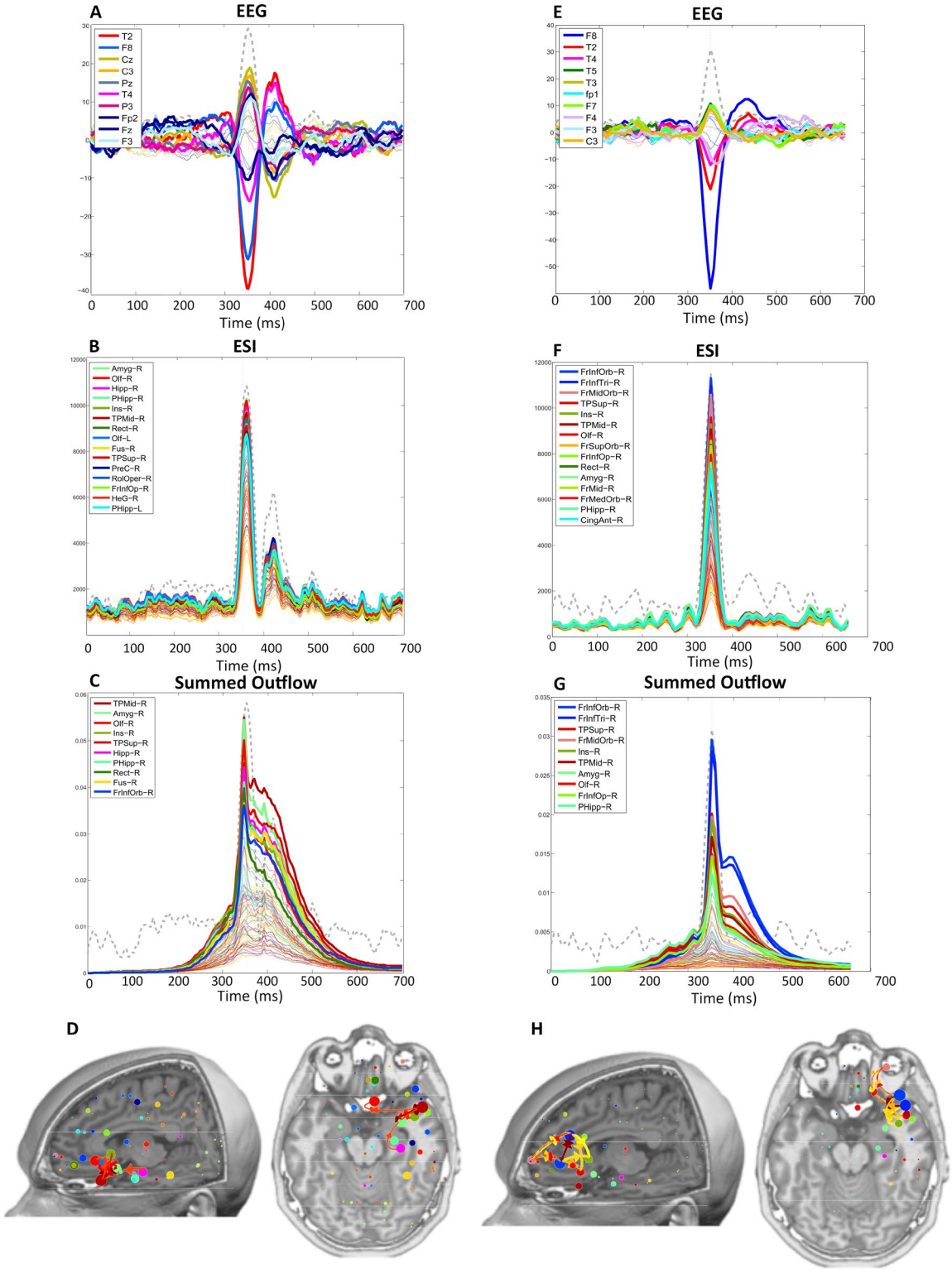

FIGURE 2 Illustrative cases of a patient (P15) with temporal lobe epilepsy (TLE (A-D) with a right temporal presumed epileptogenic zone (EZ) and an patient (P16) with extratemporal lobe epilepsy (ETLE) (E-H) with a right basal frontal presumed EZ. TLE patient: A, Electroencephalography (EEG) across time: interictal epileptiform discharges (IEDs) peak in electrode T2. B, Electrical source imaging (ESI) across time: strongest activity at the IED peak is the right amygdala. C, Summed outflow across time: maximum value at the IED peak in the right medial temporal pole. D, Summed outflow at the IED peak and strongest connections. ETLE patient E, EEG across time: IED peak in F8, (F) ESI across time: strongest region at the IED peak is the right orbital part of the inferior frontal cortex G, Summed outflow across time: maximum value at the IED peak in the right orbital part of the inferior frontal cortex and (H) summed outflow at the IED peak and strongest connections. The gray dashed lined represents the Global Field Power. L, left; R, right

TABLE 3 Relationship between incorrect EZ estimation and number of electrodes

	19 Electrodes (N = 3)	21 Electrodes (N = 13)	29 Electrodes (N = 5)	31 Electrodes (N = 11)	37 Electrodes (N = 2)
ESI	1	3	1	1	2
Summed Outflow	1	3	0	2	2
Clustering Coefficient	1	3	1	3	2
Betweenness Centrality	1	3	1	3	2
Efficiency	1	2	1	2	2

ESI, electrical source imaging; EZ, epileptogenic zone.

more widely available. A previous study using ESI based on both high-density and low-density EEG obtained a sensitivity of 84% when using individual MRI studies and high-density EEG, and a sensitivity of 66% when using low-density EEG and individual MRI studies.[3] In another study based on low-density EEG (19 channels), ESI reached a 65% concordance.[7] Another study using also low-density EEG obtained a localization accuracy of 51% and 62% using two different inverse solution methods, which was similar to other conventional neuroimaging methods (structural MRI, PET, and SPECT).[31] In our study, the percentage of concordance with the presumed EZ using ESI reached 90% in TLE and 57% in ETLE. The differences in the results may be explained by methodologic differences between the studies: different forward models (here, we used a sophisticated realistic head model including six compartments—scalp, bone, cerebral spinal fluid [CSF], gray matter, white matter, air) and inverse solutions. Moreover, the current study used cortical parcellation and regrouped gray matter solution points into regions defined by an external atlas. Therefore, the overlap with the resection zone was at the level of the atlas region and not at an individual solution point, so that the accuracy is rather assessed at a sublobar level than centimetric level. Another study also found very high sensitivity with low-density EEG.[16] That study applied ESI with identical head model and ESI algorithm but with a much higher number of automatically detected spikes (and therefore a high signal-to-noise ratio) and without brain parcellation. This suggests that several components are advantageous for a good result in low-density EEG, be it a high number of spikes, a realistic head model, or a sublobar evaluation of concordance.

This is the first study using low-density scalp EEG during interictal periods with the aim of validating DFC measures. A recent study using the ESI methodology, and a similar Granger-causality approach, demonstrated the feasibility of this procedure for EZ localization during ictal periods.[14] We demonstrate that both ESI and whole-brain directed-connectivity measures using low-density EEG during interictal spikes are able to localize the EZ with a relatively high sensitivity. We show that the regions with the highest summed outflow, clustering coefficient, betweenness centrality, and efficiency were concordant with the EZ in patients with TLE and ETLE during interictal spikes. Given that seizures might not always be detected during clinical evaluation, the use of this procedure also during interictal spikes is very relevant.

We did not see any significant difference in localization between ESI and connectivity measures. Connectivity measures did not outperform ESI, which indicates that although DFC has localization value during interictal recordings using low-density EEG, ESI might provide sufficient information for EZ localization. Nevertheless, the accuracy level of the connectivity measurement should strengthen its application to the analysis of epileptic networks and their correlation with clinical features. In two patients, ESI was discordant and connectivity measures were concordant, suggesting that connectivity could bring additional valuable information. We did not include patients with multiple foci and therefore the connectivity and ESI in such complex patients remains to be studied.

Patients with epilepsy and negative MRI represent a very difficult population in which additional localization information is very precious for presurgical evaluation. Analysis of a subgroup with negative MRI findings in independent ESI studies[4,5] or studies directly investigating ESI in MRI-negative cases[32] have shown the high accuracy of ESI in these patients using hd-EEG. Indeed, concordant ESI results were obtained in 8 of 8 (100%) with resection volume in postoperative seizure-free cases.[32] In the other study, a total concordance in patients with negative MRI result was obtained in 7 out of 11 patients (64%) and partial concordance in 4 out of 11 patients (36%).[5] The present study using low-density EEG found concordance with invasive validation (based on intracranial EEG; N = 6) together with good postoperative outcome (N = 5/6, one patient not operated) at a sublobar level in 6/6 patients with negative MRI result, so that this subgroup showed high concordance with strict invasive validation.

Both ESI and connectivity measures could significantly better localize the EZ in TLE compared to ETLE patients. Group studies have shown that patients with ETLE have worse postoperative outcome than patients with TLE,[33] and other previous studies have also shown that EZ localization in ETLE patients is more difficult than in TLE patients.[3] We obtained an accuracy of 95% for TLE and 50% for ETLE (for

the summed outflow) and 90% in TLE and 57% in ETLE (for ESI). Note that this accuracy corresponds to the overlap between atlas-based ROI and the epileptogenic lesion or resection area, thus giving an accuracy defined at a sublobar level after summarizing the whole activity of an ROI into a single time course. The anatomic limits of the ROI have no significance with respect to the extent of the estimated EZ but rather indicate that more-precise mapping could be focused around this region. In ETLE, the high level of false positives for ESI and connectivity values (43%-50%) shows that this exam could only be considered as additional information in the clinical workup and needs to be confronted to other modalities, to confirm complementary results or potentially raise additional hypotheses. Smaller brain parcels, high-density EEG,[5,34] or a very high number of spikes based on automatic detection coupled with expert selection of spikes[16,18] can improve the accuracy of ESI and ESI-based connectivity measures.

The high accuracy in TLE despite a low number of channels might be partly explained by the principally large resection zone in anterior temporal lobectomy, but also by the sophisticated head model and the sublobar level of accuracy defined by the cortical parcellation. The relationship between ESI and connectivity measures and outcome at the individual level needs to be tested in a larger study of TLE and ETLE with different surgical outcomes.

All operated patients had a good surgical outcome (inclusion criterion for validation of localization), which implies that we could not compute the specificity of our measures. Future studies should also consider patients with poor surgical outcome in order to verify the reliability of this method to identify true negatives and false positives with a well-designed measure.[35,36] The EZ estimation in non-operated patients was based on the presurgical workup (including electroclinical semiology, PET, SPECT, and intracranial EEG) as regularly used in other studies, although it is clear that invasive localization with invasive recordings followed by resection and postoperative seizure freedom remains the best comparator. In our concordance assessment, based on an atlas at the sublobar level, this non-invasive localization offers a reasonable spatial accuracy at the sublobar level.

Concerning the different number of channels, we did not find significant differences in the different types of recordings. We also did not find a significant difference between results in the recordings with fewer or more than 25 electrodes. In both patients recorded with 37 channels, the estimation was unsuccessful for all the measures, which is most likely related to a recruiting bias in our small group (both patients having had 37-channel EEG were presurgical candidates with very difficult to localize epileptic activity).

We restricted the connectivity analysis to the frequency band with the highest power at the peak of the spike as defined by the activity in the source regions. Regions with high source power will therefore appear as strong drivers if they are not strongly penalized by weak connection strength. This could explain some of the concordance between DFC and ESI. However, several regions with moderately high ESI power could also be very strong drivers if they have high connectivity strength, and notable differences between DFC and ESI should therefore be expected in such situations. Finally, the localization value of non-maximal network measures could be addressed in future studies.

The choice of the AAL atlas may have influenced the difference in results between TLE and ETLE patients for several reasons. First, the subdivision of the temporal lobe somewhat coarser than that of extratemporal areas, and this may have a negative effect on the calculation of connectivity because activity across areas with potentially different activation and connectivity is averaged. Second, there was a significant bias in that TLE surgery involved a significant higher number of AAL regions (8.4% of median brain volume in TLE vs 3.2% in ETLE), therefore providing a higher likelihood of concordance. This result suggests that such effect should be considered when estimating brain connectivity based on cortical parcellation.

We have nevertheless continued to use the AAL parcellation following our recent work[10,12,13,15] and the work of others,[37] and because the use of an atlas with clearly smaller parcels (256 or 512) is very time consuming in terms of computing the multivariate autoregressive (MVAR) models underlying the wPDC estimates. Moreover, the fact that anterior temporal lobectomies tend to comprise bigger brain areas than usually smaller extratemporal cortectomies is independent of the choice of the atlas.

In conclusion, our results show that EZ estimation with ESI and DFC using low-density EEG is feasible and could be applicable in clinical settings for helping in the diagnosis of patients with focal epilepsy. Our assessment of the localization validation of connectivity measures is promising for other applications, but larger studies with invasive validation of sensitivity and specificity are warranted.

ACKNOWLEDGMENTS

This study was funded by the Cantonal Hospital of Aarau (KSA) grant 1410.000.084. This study was also supported by the Swiss National Science Foundation (SNSF) grants 320030-169198, 163398, and CRSII5_170873, and by the Marie Sklodowska-Curie grant agreement No. 660230 (PvM).

The freely available Cartool software (https://sites.google.com/site/cartoolcommunity/) has been programmed by Denis Brunet from the Functional Brain Mapping Laboratory, Geneva, and is supported by the Center for Biomedical Imaging of Geneva and Lausanne, Switzerland.

CONFLICT OF INTEREST

PvM is a co-founder and shareholder of Epilog NV (Ghent, Belgium). MS and SV are advisors and shareholders of Epilog NV (Ghent, Belgium).
None of the other authors has any conflict of interest to disclose.

REFERENCES

1. Sillanpaa M. Long-term outcome of epilepsy. Epileptic Disord. 2000;2:79–88.
2. Michel CM, Murray MM, Lantz G, Gonzalez S, Spinelli L, Grave de Peralta R. EEG source imaging. Clin Neurophysiol. 2004;115:2195–222.
3. Brodbeck V, Spinelli L, Lascano AM, Wissmeier M, Vargas MI, Vulliemoz S, et al. Electroencephalographic source imaging: a prospective study of 152 operated epileptic patients. Brain. 2011;134:2887–97.
4. Megevand P, Spinelli L, Genetti M, Brodbeck V, Momjian S, Schaller K, et al. Electric source imaging of interictal activity accurately localises the seizure onset zone. J Neurol Neurosurg Psychiatry. 2014;85:38–43.
5. Rikir E, Koessler L, Gavaret M, Bartolomei F, Colnat-Coulbois S, Vignal JP, et al. Electrical source imaging in cortical malformation-related epilepsy: a prospective EEG-SEEG concordance study. Epilepsia. 2014;55:918–32.
6. Maliia MD, Meritam P, Scherg M, Fabricius M, Rubboli G, Mîndruţă I, et al. Epileptiform discharge propagation: analyzing spikes from the onset to the peak. Clin Neurophysiol. 2016;127:2127–33.
7. Russo A, Jayakar P, Lallas M, Miller I, Hyslop A, Korman B, et al. The diagnostic utility of 3D electroencephalography source imaging in pediatric epilepsy surgery. Epilepsia. 2016;57:24–31.
8. Laufs H. Functional imaging of seizures and epilepsy: evolution from zones to networks. Curr Opin Neurol. 2012;25:194–200.
9. Richardson MP. Large scale brain models of epilepsy: dynamics meets connectomics. J Neurol Neurosurg Psychiatry. 2012;83:1238–48.
10. Coito A, Michel CM, van Mierlo P, Vulliemoz S, Plomp G. Directed functional brain connectivity based on EEG source imaging: methodology and application to temporal lobe epilepsy. IEEE Trans Biomed Eng. 2016;63:2619–28.
11. Granger CWJ. Investigating causal relations by econometric models and cross-spectral methods. Econometrica. 1969;37:424–38.
12. Coito A, Plomp G, Genetti M, Abela E, Wiest R, Seeck M, et al. Dynamic directed interictal connectivity in left and right temporal lobe epilepsy. Epilepsia. 2015;56:207–17.
13. Coito A, Genetti M, Pittau F, Iannotti GR, Thomschewski A, Höller Y, et al. Altered directed functional connectivity in temporal lobe epilepsy in the absence of interictal spikes: a high density EEG study. Epilepsia. 2016;57:402–11.
14. Staljanssens W, Strobbe G, Van Holen R, Keereman V, Gadeyne S, Carrette E, et al. EEG source connectivity to localize the seizure onset zone in patients with drug resistant epilepsy. Neuroimage Clin. 2017;16:689–98.
15. Coito A, Michel CM, Vulliemoz S, Plomp G. Directed functional connections underlying spontaneous brain activity. Hum Brain Mapp. 2019;40:879–88.
16. van Mierlo P, Strobbe G, Keereman V, Birot G, Gadeyne S, Gschwind M, et al. Automated long-term EEG analysis to localize the epileptogenic zone. Epilepsia Open. 2017;2:322–33.
17. Pascual-Marqui RD. Standardized low-resolution brain electromagnetic tomography (sLORETA): technical details. Methods Find Exp Clin Pharmacol. 2002;24(suppl 1):5–12.
18. Baroumand AG, van Mierlo P, Strobbe G, Pinborg LH, Fabricius M, Rubboli G, et al. Automated EEG source imaging: a retrospective, blinded clinical validation study. Clin Neurophysiol. 2018;129:2403–10.
19. Gschwind M, van Mierlo P, Ruegg S. Little effort with big effect - implementing the new IFCN 2017 recommendations on standard EEGs. Clin Neurophysiol. 2018;129:2433–4.
20. Tzourio-Mazoyer N, Landeau B, Papathanassiou D, Crivello F, Etard O, Delcroix N, et al. Automated anatomical labeling of activations in SPM using a macroscopic anatomical parcellation of the MNI MRI single-subject brain. NeuroImage. 2002;15:273–89.
21. Stockwell RGM, Lowe RP. Localization of the complex spectrum: the S Transform. IEEE Trans Signal Process. 1996;44:998–1001.
22. Baccala LA, Sameshima K. Partial directed coherence: a new concept in neural structure determination. Biol Cybern. 2001;84:463–74.
23. Astolfi L, Cincotti F, Mattia D, Tocci A, Colosimo A, Salinari S, et al. Tracking the time-varying cortical connectivity patterns by adaptive multivariate estimators. IEEE Trans Bio-Med Eng. 2008;55:902–13.
24. Plomp G, Quairiaux C, Michel CM, Astolfi L. The physiological plausibility of time-varying Granger-causal modeling: normalization and weighting by spectral power. NeuroImage. 2014;97:206–16.
25. Moller E, Schack B, Arnold M, Witte H. Instantaneous multivariate EEG coherence analysis by means of adaptive high-dimensional autoregressive models. J Neurosci Methods. 2001;105:143–58.
26. Hesse W, Moller E, Arnold M, Schack B. The use of time-variant EEG Granger causality for inspecting directed interdependencies of neural assemblies. J Neurosci Methods. 2003;124:27–44.
27. Astolfi L, Cincotti F, Mattia D, Marciani MG, Baccala L, De Vico Fallani F, et al. Assessing cortical functional connectivity by partial directed coherence: simulations and application to real data. IEEE Trans Bio-Med Eng. 2006;53:1802–12.
28. Bullmore E, Sporns O. Complex brain networks: graph theoretical analysis of structural and functional systems. Nat Rev Neurosci. 2009;10:186–98.
29. Rubinov M, Sporns O. Complex network measures of brain connectivity: uses and interpretations. NeuroImage. 2010;52:1059–69.
30. Verhoeven T, Coito A, Plomp G, Thomschewski A, Pittau F, Trinka E, et al. Automated diagnosis of temporal lobe epilepsy in the absence of interictal spikes. Neuroimage Clin. 2018;17:10–5.
31. Sharma P, Scherg M, Pinborg LH, Fabricius M, Rubboli G, Pedersen B, et al. Ictal and interictal electric source imaging in pre-surgical evaluation: a prospective study. Eur J Neurol. 2018;25:1154–60.
32. Brodbeck V, Spinelli L, Lascano AM, Pollo C, Schaller K, Vargas MI, et al. Electrical source imaging for presurgical focus localization in epilepsy patients with normal MRI. Epilepsia. 2010;51:583–91.
33. de Tisi J, Bell GS, Peacock JL, McEvoy AW, Harkness HWJ, Sander JW, et al. The long-term outcome of adult epilepsy surgery,

patterns of seizure remission, and relapse: a cohort study. Lancet. 2011;378:1388–95.
34. Lascano AM, Perneger T, Vulliemoz S, Spinelli L, Garibotto V, Korff CM, et al. Yield of MRI, high-density electric source imaging (HD-ESI), SPECT and PET in epilepsy surgery candidates. Clin Neurophysiol. 2016;127:150–5.
35. Rikir E, Koessler L, Ramantani G, Maillard LG. Added value and limitations of electrical source localization. Epilepsia. 2017;58:174–5.
36. Lantz G, Spinelli L, Seeck M, de Peralta Menendez RG, Sottas CC, Michel CM. Propagation of interictal epileptiform activity can lead to erroneous source localizations: a 128-channel EEG mapping study. J Clin Neurophysiol. 2003;20:311–9.
37. Adebimpe A, Bourel-Ponchel E, Wallois F. Identifying neural drivers of benign childhood epilepsy with centrotemporal spikes. Neuroimage Clin. 2018;17:739–50.

SUPPORTING INFORMATION

Additional supporting information may be found online in the Supporting Information section at the end of the article.

How to cite this article: Coito A, Biethahn S, Tepperberg J, et al. Interictal epileptogenic zone localization in patients with focal epilepsy using electric source imaging and directed functional connectivity from low-density EEG. *Epilepsia Open*. 2019;4:281–292. https://doi.org/10.1002/epi4.12318